Biochemical and Biophysical Research Communications 388 (2009) 86–90

Contents lists available at ScienceDirect

Biochemical and Biophysical Research Communications

journal homepage: www.elsevier.com/locate/ybbrc

Mixed modes in opening of KcsA potassium channel from a targeted molecular dynamics simulation

Wenyu Zhong, Wanlin Guo *

Institute of Nano Science, Nanjing University of Aeronautics and Astronautics, Nanjing, 210016, China

ARTICLE INFO

Article history:
Received 22 July 2009
Available online 29 July 2009

Keywords:
Potassium channel
Gating
Molecular dynamics
Simulation
KcsA
Kv1.2

ABSTRACT

Potassium channels conduct K^+ flow selectively across the membrane through a central pore. During a process called gating, the potassium channels undergo a conformational change that opens or closes the ion-conducting pore. The potassium channel KcsA has been structurally determined in its closed state. However, the dynamic mechanism of the gating transition of the KcsA channel is still being investigated. Here, a targeted molecular dynamics simulation up to 150 ns is performed to investigate the detailed opening process of the KcsA channel with an open Kv1.2 structure serving as the target. The channel arrived at a self-determined quasi-stable state within 60 ns. The rigid-body and hinge-bending modes are observed mixed together in the remaining 90 ns long quasi-stable state. The mixed-mode movement seems come from the competition between the helix rigidity and the biased-applied gating force.

Potassium channels are transmembrane proteins that conduct K^+ flux selectively across the membrane through a central pore. In a process called gating, these channels open or close the central pore to control the K^+ flux. The first determined X-ray crystallographic structure of the potassium channel, KcsA from *Streptomyces lividans* [1] (Fig. 1A), provides important structural information for understanding the functional mechanism of potassium channels. It is composed of four identical subunits of two transmembrane helices (the outer-helix M1 and the inner-helix M2) linked by a re-entrant loop, dispersed symmetrically around a common axis corresponding to the central pore. The pore can be divided into three parts: a selectivity filter near the extracellular side, a dilated water-filled cavity at the center, and a closed gate near the cytoplasmic side formed by four packed M2 helices. This architecture is found to be highly conserved in the potassium channel family [2,3], including both the eukaryotic and prokaryotic ones. KcsA has becomes the most extensively studied potassium channel, and is widely used as the template in potassium channel research [4]. Although KcsA was proved to open at acidic pH [5–8], the open state of KcsA and the dynamical mechanism underlying its gating process is still being investigated.

During the opening process, the M2 helices have to be moved apart to open the intracellular gate. There are currently two competing models for how the M2 helices are moved during the opening process. Studies of KcsA using the spin-labeling method and electron paramagnetic resonance (EPR) spectroscopy suggested that the opening is accomplished by a rigid-body tilting motion of M2 [9,10] (the EPR model is shown in Fig. 1C). In contrast, structural comparison between KcsA and an open channel, MthK, suggested a hinge-bending motion [11], where the opening is accomplished by an outward bend of M2 at a glycine hinge. Therefore, how the M2 helix moves or deforms during KcsA opening remains under study. Recently, several works have supported the hinge-bending model. Similar bending motions to those of the inner-helices are observed in two determined open channels, KvAP [12] at a glycine hinge and Kv1.2 [13] (Fig. 1B) at a PVP sequence hinge. Experimental studies [14,15] of KcsA also provide positive evidence for the hinge-bending model. However, using Monte Carlo normal mode following simulations, Miloshevsky and Jordan have suggested that both modes exist in the opening process of KcsA [16]. They have demonstrated that the two modes illuminate different stages in gating: the transition begins with rigid-body tilting of M2 and ends at a final state with M2 being bent. Although these studies yield a wealth of information, channel gating is intrinsically a dynamic process and more dynamical considerations are necessary to understand the underlying mechanism.

Molecular dynamics (MD) methods are powerful simulation tools for representation of the dynamic development of a complex biological macromolecular system [17]. Unfortunately, the time scale of the gating process is in the order of microseconds, which is still far beyond the current computational capability. Steered MD (SMD) [18] and targeted MD (TMD) simulations [19] were performed to represent the opening process of KcsA. However, these simulations are completed in no more than 10 ns simulation times with large artificial forces. Although valuable information has been derived, most detailed information is missed.

* Corresponding author. Fax: +86 25 84895827.
E-mail address: wlguo@nuaa.edu.cn (W. Guo).

0006-291X/$ - see front matter © 2009 Elsevier Inc. All rights reserved.
doi:10.1016/j.bbrc.2009.07.123

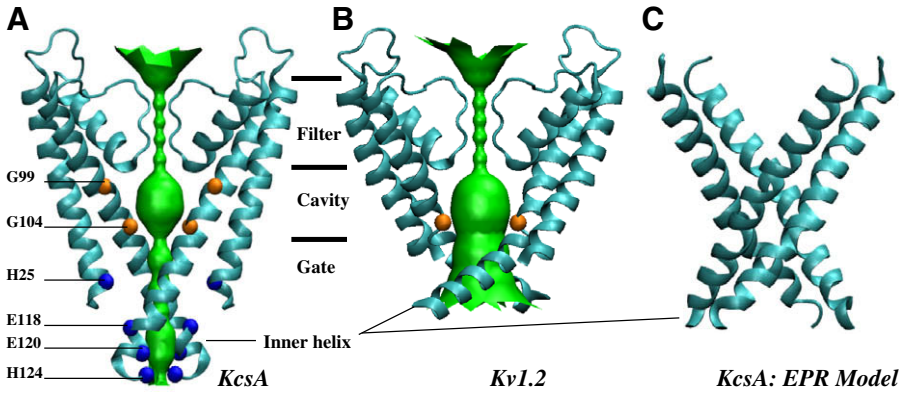

Fig. 1. Structures of KcsA and Kv1.2 K^+ channel. (A) KcsA and its pore profile. The potential hinge residues (orange) and pH-sensing residues (blue) are labeled. (B) Kv1.2 and its pore profile. The hinge is labeled in orange. (C) The EPR model of the inner-helices of KcsA. For clarity, only two opposite subunits are shown in (A) and (B). (For interpretation of the references to color in this figure legend, the reader is referred to the web version of this article.)

Here we represent the dynamic opening process of the KcsA K^+ channel using a long time TMD simulation of up to 150 ns with the Kv1.2 core structure serving as the targeted conformation. The four subunits are observed to move in an asymmetrical manner, where both rigid-body moving and hinge-bending modes exist simultaneously and make comparable contributions to channel gating. Further analysis show that the competition between the helix rigidity and the biased-applied gating forces resulted the mixed-mode movement.

Methods

The total number of atoms in the simulation system is 45,377, including the KcsA structure containing 6324 atoms (PDB code 1K4C, Ref. [20], shown in Fig. 1A), 119 DMPC (dimyristoyl phosphatidylcholine) lipid molecules, 8317 water molecules, and 20 K^+ and 40 Cl^- ions. The system is electronically neutral.

The protein (residues 22–124) is acetylated on the N-terminus and methylated on the C-terminus to mimic the preceding peptide bond. His^{25} and His^{124} are protonated to simulate an weakly acidic environment as the intracellular gate of KcsA can be 50% open at pH 5.3 [8], and Glu^{71} is constructed in a protonated state as in previous works [21,22], while the others are in their default states. The coordinates of hydrogen atoms are constructed using the plug-in Psfgen of the visual program VMD [23]. The protein is embedded into the solvated DMPC bilayer. The membrane normal and the protein pore are oriented along the Z axis. Two K^+ ions are placed in the selectivity filter (at the binding sites 1 and 3, respectively) and one is placed in the cavity, according to Ref. [20].

Energy minimization and molecular dynamics relaxing (longer than 9 ns in total) in NVT or NPT ensembles are repeated with progressively decreasing restraints on the protein atoms [24]. The modeling procedures mainly refer to our previous work [25]. The equilibrated simulation box dimensions are 73 Å × 73 Å × 82 Å. A productive TMD simulation of up to 150 ns is thus performed in a NVT ensemble, which is initiated from the last frame of the equilibration.

The targeted molecular dynamics approach used here is different from the classical one [26], but similar to that used in Refs. [19,25]. The Kv1.2 structure (PDB code 2A79, Ref. [13], shown in Fig. 1B) is used to serve as the targeted open conformation in the TMD simulation. Peptide N, C, and C_α atoms of the two transmembrane helices of KcsA (residues 25–50 and 86–122) are restrained to the corresponding positions of Kv1.2 (residues 324–349 and 385–421) with harmonic potential of $k = 0.003$ kcal·mol^{-1}·Å^{-2} per atom. The backbone of the selectivity filter is restrained with a harmonic potential of $k = 1$ kcal·mol^{-1}·Å^{-2} to avoid protein drift. The relative positions of the two proteins in both the residue sequence and Cartesian space are aligned by matching the selector of KcsA (residues 75–79) to the selector of Kv1.2 (residues 374–378).

All the MD simulations are performed with the program NAMD [27] using the CHARMM27 force field for protein and lipids [28]. The CHARMM-modified [28] TIP3P model [29] is used for water. The van der Waals interactions are smoothly switched off in the range of 8–10 Å. The electrostatic interactions are computed without cut-off using the particle mesh Ewald (PME) method [30]. The SHAKE and SETTLE algorithms [31] are used to fix the length of all bonds involving hydrogen atoms, and an integration time step of 2 fs is used. The temperature coupling method is used to keep the temperature constant at 310 K with a coupling factor of 1.0 ps^{-1}. A Langevin piston method [32,33] is used to maintain a constant pressure of 1 bar in the NPT ensemble with a decay period of 200 fs and a damping period of 100 fs.

To quantify the hinge-bending mode, the hinge location and bending angle of a helix which refer to its initial state, as shown in Fig. 3D, should be determined. Here we use a weighted average Root-Mean-Square-Deviation (RMSD) of a bent helix relative to the original inner-helix of KcsA to determine the hinge location. The weighted average RMSD ($RMSD_{WA}$) is calculated as

$$RMSD_{WA} = [(i - a)RMSD_{D1} + (b - i)RMSD_{D2}]/(b - a)$$

where a and b are assumed to be 86 and 122, respectively, denoting the residue numbers of each end of the helix, and i denotes the number of a candidate hinge residue. D1 and D2 denote the two domains of the helix partitioned by the candidate hinge. Each domain contains at least 10 residues. $RMSD_{D1}$ and $RMSD_{D2}$ denote the C_α, peptide N and C RMSD values of the two domains relative to the original M2 helix of KcsA after least-squares superposition. The candidate residue with the smallest $RMSD_{WA}$ is chosen to be the hinge location. The bending angle is then determined by the angle between the principal axes of inertia of the two domains separated by the hinge.

The tilting angle, as shown in Fig. 3D, used to quantify the rigid-body moving mode is also determined by the principal axes of inertia. To avoid interference from the hinge-bending mode, only the upper-half of the domain (residue 86–102) is used in the calculation.

The HOLE program [34] is used to calculate the pore radius profiles. Structural diagrams are prepared using VMD[23].

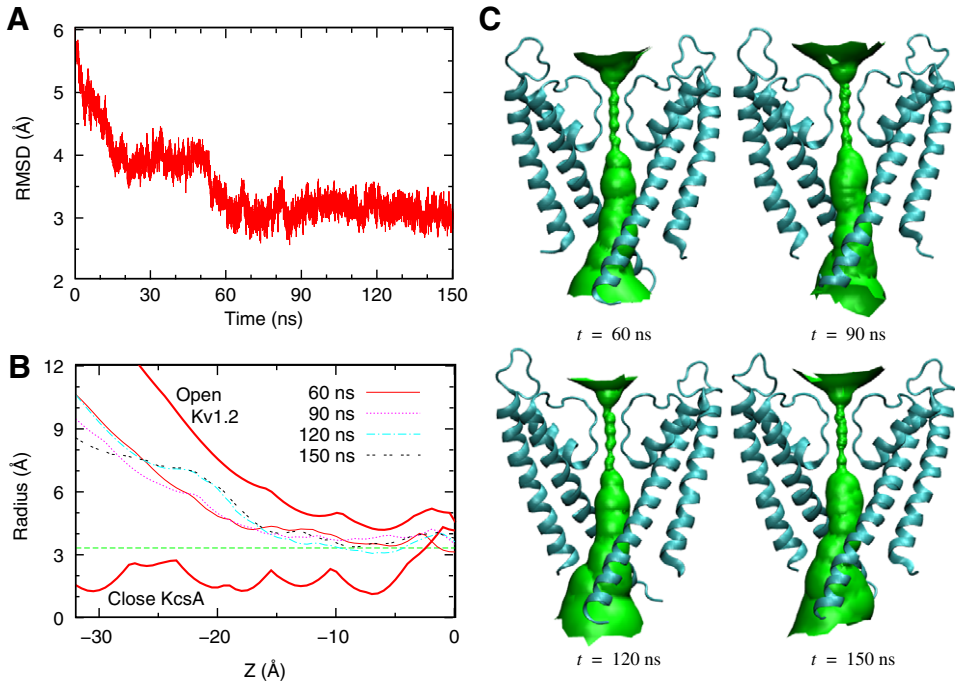

Fig. 2. (A) The C_α RMSD of the inner-helices (residues 86–120) between the KcsA structure in the simulation and the crystal structure of Kv1.2. (B) The radius profiles at the gate region from snapshots of the channel at $t = 60$, 90, 120 and 150 ns, while the profiles of crystal structures of KcsA and Kv1.2 are presented for reference. (C) The structure and pore profile of the KcsA in opening at $t = 60$, 90, 120 and 150 ns.

Results and discussion

A simple measurement of the opening process is provided by the RMSD between the channel structure at a given time and the targeted open structure. The C_α RMSD of M2, drawn in Fig. 2A, decreases monotonically during the first 60 ns of the simulation, but remains stable for the last 90 ns of the 150 ns simulation. This shows that the opening process continues to $t = 60$ ns, and then stagnates. The radius profiles of the pore of selected snapshots at $t = 60$, 90, 120 and 150 ns, drawn in Fig. 2B–C, also show that the protein achieved a partial opening, or quasi-opening state. During the final 90 ns, the radius profiles show very slight changes at the intracellular entryway. The gate becomes wide enough to pass a hydrated K^+ with radius assumed to be 3.3 Å, but is not as wide as that in the open Kv1.2 structure. The observed opening process is associated with the constant spring coefficient used for the restraints. When the protein approaches the targeted structure, the applied spring forces become weaker and weaker, and finally lose the ability to drive the protein for further targeted movements. Thus some native information, including the moving mode of M2, could be drawn from the final 90 ns quasi-opening structure, as the restraint spring forces are very weak.

Time-averaged structures of the protein for every 10 ns of the last 90 ns are used in the analysis to exclude the influence of thermal fluctuation. The method for determination of the hinge location and the bending angle of the hinge-bending mode, and the tilting angle of the rigid-body mode, has been described in the Method section. The angles are summarized in Fig. 3A–B, and the hinge locations are summarized in Table 1. The statistical scatter in the hinge location, and the bending and tilting angles presented in Fig. 3A–B shows that the channel continues searching for an optimum conformation for the M2 helices, although the opening magnitude is maintained by the weak restraint spring force. However, the movement of M2 becomes smaller and smaller in the quasi-opening state, showing that the channel is approaching an optimum state. Both the rigid-body and hinge-bending moving modes are observed. The M2 helices of the four subunits exhibit complex and asymmetrical movements. Their contributions to channel opening are summarized in Fig. 3C. Because Thr^{107} is the key residue for pore opening and forms the narrowest region of the gate, as shown in the embedded figures in Fig. 3C, the radius increment of the Thr^{107} C_α atom is used to represent the contribution of each subunit. Here, the radius increment is defined as the increment of the distance from the pore axis relative to that of the original structure. For reference, the radius increment of the Thr^{107} C_α atom in the Kv1.2 conformation is 5.2 Å with a bending angle of about 30° and in the EPR model of KcsA it is 4.5 Å with a tilting angle of about 8°.

Subunit A exhibits a slight hinge-bending and a decreasing rigid-body moving mode, with bending angles of about 5° for all and tilting angles ranging between 2° and 3.5°. The radius increment decreased from about 2.5 Å to 1.8 Å. Subunit B undergoes a mode transition from hinge-bending to rigid-body movement, with the bending angles decreasing from about 12° to 4° and the tilting angles increasing from about 1.5° to 6.2°. During the mode transition, the contribution of subunit B to the channel opening increases and ultimately becomes the largest one, with a radius increment of 2.8 Å. Subunit C undergoes the most obvious hinge-bending movement and rigid-body movement, with bending angle of up to 28° and tilting angle up to 6.1°. Finally, it becomes the largest bending mode contributor and the second largest rigid mode contributor, and overall the second largest contributor to the opening. Subunit D exhibits an obvious and increasing hinge-bending mode and a slight and decreasing rigid-body mode. In contrast to subunit B, subunit D switches from a mixed hinge-bending and rigid-body mode to a hinge-bending dominated mode, with an increasing radius increment.

As shown in Table 1, the hinge locations of the M2 helices of the time-averaged structures are gathering to the two glycine residues. Thirty of the thirty-six hinges, and all of the four final hinges, locate between Gly^{99} and Gly^{104}. The observation is in good agreement with the glycine hinge proposal [11].

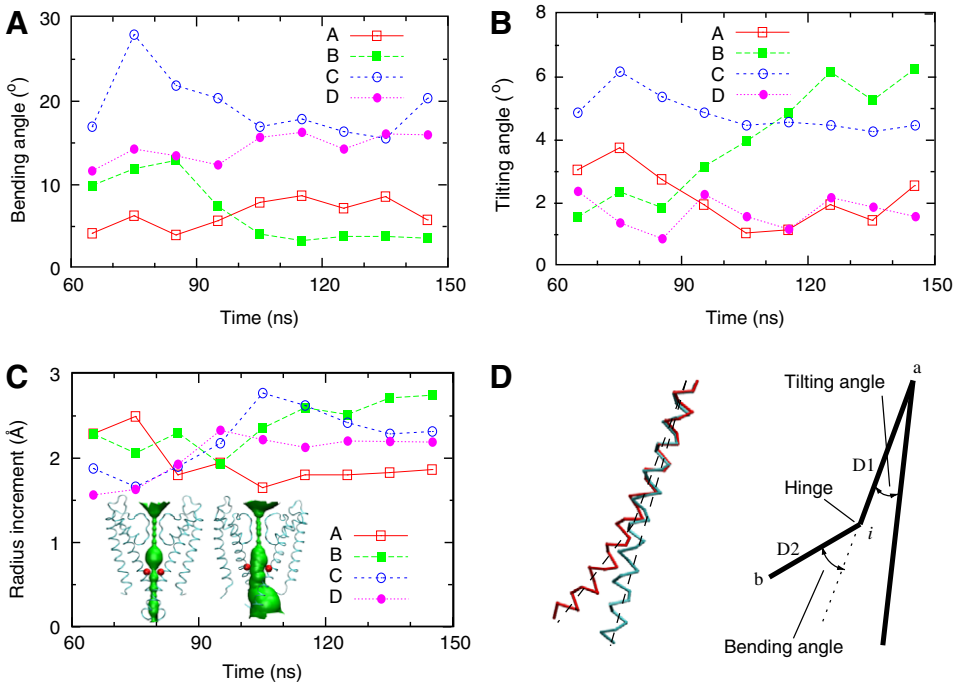

Fig. 3. Bending angle, tilting angle and radius increments of each subunit of the time-averaged structures over 10 ns duration at each point. (A) Bending angles. (B) Tilting angles. (C) Increments relative to the KcsA crystal structure of the distance of the Thr^{107} C_α atom to the pore axis. (D) Schematic diagram of the hinge-bending and rigid-body moving mode of a helix.

Table 1
Hinge locations of each subunit of the time-averaged structures.

Time	A	B	C	D
60–70	Gly^{104}	Ile^{100}	Phe^{103}	Gly^{104}
70–80	Val^{97}	Gly^{99}	Val^{106}	Gly^{104}
80–90	Leu^{105}	Ile^{100}	Phe^{103}	Gly^{104}
90–100	Gly^{104}	Gly^{99}	Gly^{99}	Ile^{100}
100–110	Ile^{100}	Ile^{100}	Thr^{101}	Ile^{100}
110–120	Ala^{98}	Gly^{99}	Ile^{100}	Phe^{103}
120–130	Leu^{110}	Gly^{99}	Thr^{101}	Thr^{101}
130–140	Ala^{111}	Gly^{99}	Thr^{101}	Phe^{103}
140–150	Thr^{101}	Gly^{99}	Ile^{100}	Ile^{100}

The above results show that the M2 helices undergo a mixed-mode movement, in which the rigid-body mode and hinge-bending mode could exist simultaneously and exchange between each other. Here we would like to suggest that the mixed-mode movement is come from the competition between the intrinsic rigidity of the helix and the applied gating forces. Although a helix with glycine residues can adopt flexible conformations, it will still more favor a rigidity conformation by the helix itself. On the other hand, the gating forces in the simulation, including both the spring forces and the electrical repulsion forces between the protonated histidine residues, will favor a bending conformation. Because the spring forces are targeted to the bending inner-helices of Kv1.2, and the electrical forces are biased applied on M2, as His^{25} and His^{124} located far below the glycine hinge (shown in Fig. 1).

Actually, gating forces in pH-gated experiments of KcsA are all biased applied on M2, as all potential pH-sensing residues, including His^{25}, Glu^{118}, Glu^{120} and His^{124} [7,8], located below the glycine residues (shown in Fig. 1). Therefore the competition of the two moving modes will also exist, and the mixed-mode movement of M2 could be applied in experimental cases. On a speculative note, it is possible that the bent M2 of KcsA observed in Refs. [14,15] indicate final victories of the gating forces, and the KcsA opening begins with M2 tilting and ends at M2 bending [16] should reflect to the transferring of the competitive advantage from helix rigidity to gating forces.

Conclusion

Using the open Kv1.2 structure to serve as the targeted conformation, the opening process of the KcsA K^+ channel is investigated from its initial closed state through a 150 ns long targeted molecular dynamics simulation. The channel arrived at a partially open, quasi-stable state, within the first 60 ns of the simulation. The quasi-stable state is optimized by the intrinsic properties of the channel, and lasts for the remaining 90 ns of the simulation, providing detailed information for the moving mode of the inner-helix during the closed-open transition of KcsA. Both the rigid-body and hinge-bending modes are observed simultaneously and make comparable contributions to the opening of the KcsA channel. The competing between the intrinsic rigidity of the helix and the gating forces, seems to be responsible for the mixed-mode movement. Thus the mixed-mode movement of KcsA opening could be universal in the pH-gated experiments of KcsA.

Acknowledgments

The work is supported by National NSF (No. 10802037 and No. 10732040) of China, Jiangsu Planned Projects for Postdoctoral Research Funds (No. 0802015C) and NSF (No. BK2008042) of Jiangsu Province.

References

[1] D.A. Doyle, J.H. Morais Cabral, R.A. Pfuetzner, A. Kuo, J.M. Gulbis, S.L. Cohen, B.T. Chait, R. MacKinnon, The structure of the potassium channel: molecular basis of K^+ conduction and selectivity, Science 280 (1998) 69–77.
[2] Z. Lu, A.M. Klem, Y. Ramu, Ion conduction pore is conserved among potassium channels, Nature 413 (2001) 809–813.
[3] S. Choe, Potassium channel structures, Nat. Rev. Neurosci. 3 (2002) 115–121.
[4] B. Roux, Ion conduction and selectivity in K^+ channels, Annu. Rev. Biophys. Biomol. Struct. 34 (2005) 153–171.

[5] L. Cuello, J. Romero, D. Cortes, E. Perozo, pH-dependent gating in the *Streptomyces lividans* K^+ channel, Biochemistry 37 (1998) 3229–3236.
[6] L. Heginbotham, M. LeMasurier, L. Kolmakova-Partensky, C. Miller, Single *Streptomyces lividans* K^+ channels: functional asymmetries and sidedness of proton activation, J. Gen. Physiol. 114 (1999) 551–560.
[7] D.M. Cortes, L.G. Cuello, E. Perozo, Molecular architecture of full-length KcsA: role of cytoplasmic domains in ion permeation and activation gating, J. Gen. Physiol. 117 (2001) 165–180.
[8] A.N. Thompson, D.J. Posson, P.V. Parsa, C.M. Nimigean, Molecular mechanism of pH sensing in KcsA potassium channels, Proc. Natl. Acad. Sci. USA 105 (2008) 6900–6905. PMID: 18443286.
[9] E. Perozo, D.M. Cortes, L.G. Cuello, Structural rearrangements underlying K^+-channel activation gating, Science 285 (1999) 73–78.
[10] Y.-S. Liu, P. Sompornpisut, E. Perozo, Structure of the KcsA channel intracellular gate in the open state, Nat. Struct. Biol. 8 (2001) 883–887.
[11] Y. Jiang, A. Lee, J. Chen, M. Cadene, B.T. Chait, R. MacKinnon, The open pore conformation of potassium channels, Nature 417 (2002) 523–526.
[12] Y. Jiang, A. Lee, J. Chen, V. Ruta, M. Cadene, B.T. Chait, R. MacKinnon, X-ray structure of a voltage-dependent K^+ channel, Nature 423 (2003) 33–41.
[13] S.B. Long, E.B. Campbell, R. Mackinnon, Crystal structure of a mammalian voltage-dependent *Shaker* family K^+ channel, Science 309 (2005) 897–903.
[14] B.L. Kelly, A. Gross, Potassium channel gating observed with site-directed mass tagging, Nat. Struct. Biol. 10 (2003) 280–284.
[15] H. Shimizu, M. Iwamoto, T. Konno, A. Nihei, Y.C. Sasaki, S. Oiki, Global twisting motion of single molecular KcsA potassium channel upon gating, Cell 132 (2008) 67–78.
[16] G.V. Miloshevsky, P.C. Jordan, Open-state conformation of the KcsA K^+ channel: Monte Carlo normal mode following simulations, Structure 15 (2007) 1654–1662.
[17] M. Karplus, J.A. McCammon, Molecular dynamics simulations of biomolecules, Nat. Struct. Biol. 9 (2002) 646–652.
[18] P.C. Biggin, M.S.P. Sansom, Open-state models of a potassium channel, Biophys. J. 83 (2002) 1867–1876.
[19] M. Compoint, F. Picaud, C. Ramseyer, C. Girardet, Targeted molecular dynamics of an open-state KcsA channel, J. Chem. Phys. 122 (2005) 134707.
[20] Y. Zhou, J.H. Morais-Cabral, A. Kaufman, R. MacKinnon, Chemistry of ion coordination and hydration revealed by a K^+ channel-Fab complex at 2.0 Å resolution, Nature 414 (2001) 43–48.
[21] K.M. Ranatunga, I.H. Shrivastava, G.R. Smith, M.S.P. Sansom, Side-chain ionization states in a potassium channel, Biophys. J. 80 (2001) 1210–1219.
[22] S. Berneche, B. Roux, The ionization state and the conformation of Glu-71 in the KcsA K^+ channel, Biophys. J. 82 (2002) 772–780.
[23] W. Humphrey, A. Dalke, K. Schulten, VMD: visual molecular dynamics, J. Mol. Graph. 14 (1996) 33–38.
[24] S. Berneche, B. Roux, Molecular dynamics of the KcsA K^+ channel in a bilayer membrane, Biophys. J. 78 (2000) 2900–2917.
[25] W. Zhong, W. Guo, S. Ma, Intrinsic aqueduct orifices facilitate K^+ channel gating, FEBS Lett. 582 (2008) 3320–3324.
[26] J. Schlitter, M. Engels, P. Kruger, Targeted molecular dynamics: a new approach for searching pathways of conformational transitions, J. Mol. Graph. 12 (1994) 84–89.
[27] J.C. Phillips, R. Braun, W. Wang, J. Gumbart, E. Tajkhorshid, E. Villa, C. Chipot, R.D. Skeel, L. Kale, K. Schulten, Scalable molecular dynamics with NAMD, J. Comput. Chem. 26 (2005) 1781–1802.
[28] A. MacKerell, D. Bashford, M. Bellott, R. Dunbrack, J. Evanseck, M. Field, S. Fischer, J. Gao, H. Guo, S. Ha, D. Joseph-McCarthy, L. Kuchnir, K. Kuczera, F. Lau, C. Mattos, S. Michnick, T. Ngo, D. Nguyen, B. Prodhom, W. Reiher, B. Roux, M. Schlenkrich, J. Smith, R. Stote, J. Straub, M. Watanabe, J. Wiorkiewicz-Kuczera, D. Yin, M. Karplus, All-atom empirical potential for molecular modeling and dynamics studies of proteins, J. Phys. Chem. B 102 (1998) 3586–3616.
[29] W.L. Jorgensen, J. Chandrasekhar, J.D. Madura, R.W. Impey, M.L. Klein, Comparison of simple potential functions for simulating liquid water, J. Chem. Phys. 79 (1983) 926–935.
[30] U. Essmann, L. Perera, M.L. Berkowitz, T. Darden, H. Lee, L.G. Pedersen, A smooth particle mesh Ewald method, J. Chem. Phys. 103 (1995) 8577–8593.
[31] S. Miyamoto, P.A. Kollman, Settle: an analytical version of the SHAKE and RATTLE algorithm for rigid water models, J. Comput. Chem. 13 (1992) 952–962.
[32] G.J. Martyna, D.J. Tobias, M.L. Klein, Constant pressure molecular dynamics algorithms, J. Chem. Phys. 101 (1994) 4177–4189.
[33] S.E. Feller, Y. Zhang, R.W. Pastor, B.R. Brooks, Constant pressure molecular dynamics simulation: the Langevin piston method, J. Chem. Phys. 103 (1995) 4613–4621.
[34] O.S. Smart, J.M. Goodfellow, B.A. Wallace, The pore dimensions of gramicidin A, Biophys. J. 65 (1993) 2455–2460.